

Supporting Information

Bionic dual-scale structured films for efficient passive radiative cooling accompanied by robust durability

Renwei Zhang, Ningning Sun, Zehong Zhao, Shixu Wang, Mengfan Zhang, Lei Zhao, Yahua Liu
and Shile Feng*

State Key Laboratory of High-performance Precision Manufacturing, Dalian University of
Technology, Dalian 116024, P. R. China

Corresponding author: fengshile@dlut.edu.cn

This file includes:

Section 1. Supplementary Figures S1 to S13

Section 2. Supplementary Video S1

Section 1. Supplementary Figure S1 to S13

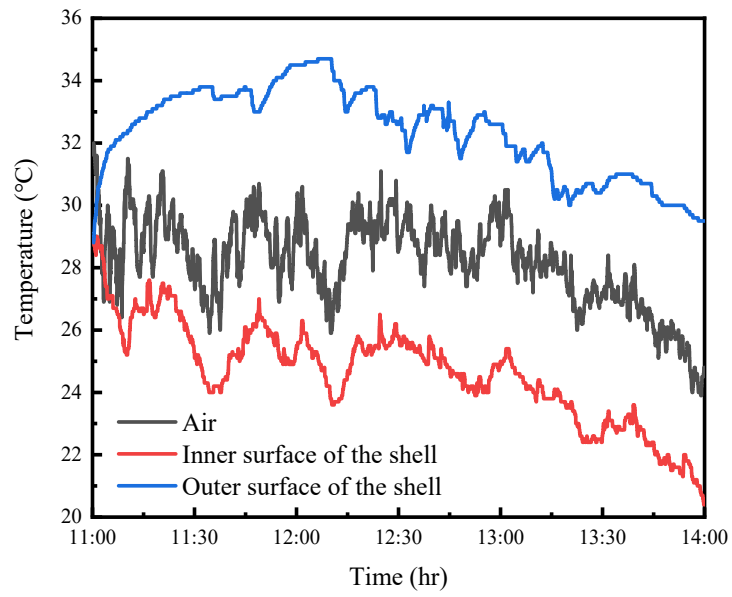


Figure S1: Cooling test of the inner and outer surfaces of the *Hawaiian scallop* shell.

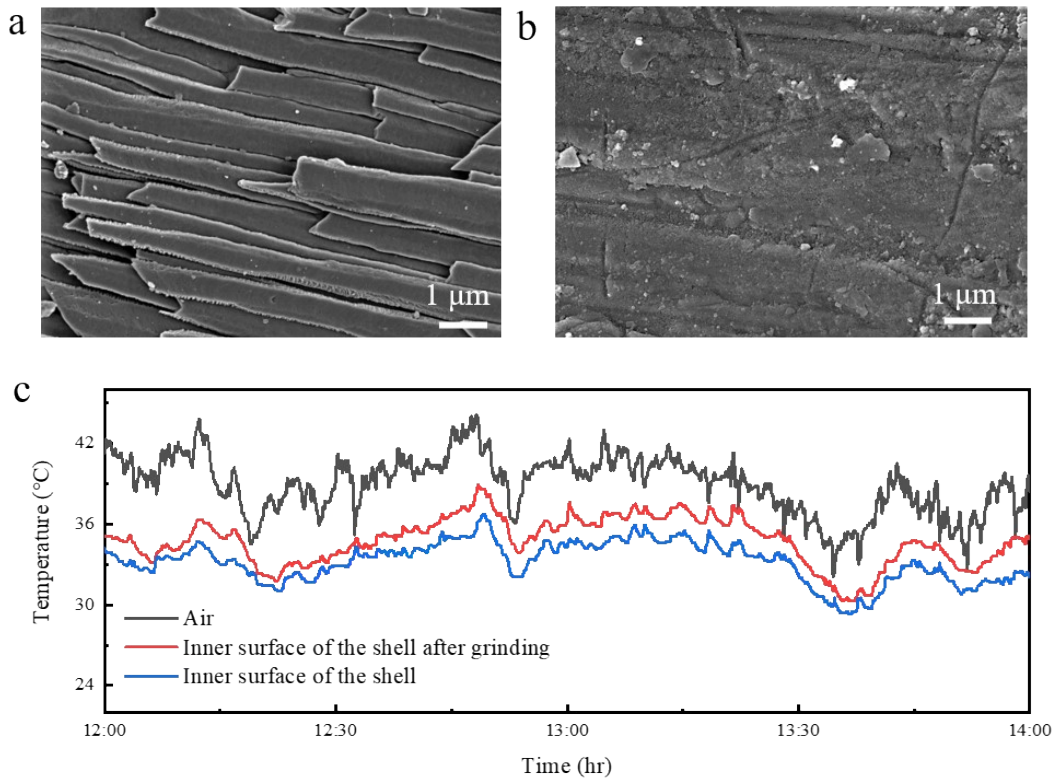


Figure S2: SEM images and cooling tests of the inner surface before and after grinding. (a) SEM image of the inner surface of the shell before grinding. (b) SEM image of the inner surface of the shell after grinding. (c) Cooling tests of the inner surface of shells before and after grinding. To eliminate the influence of environmental factors on the testing site, two adjacent areas of the same shell were selected for the cooling test.

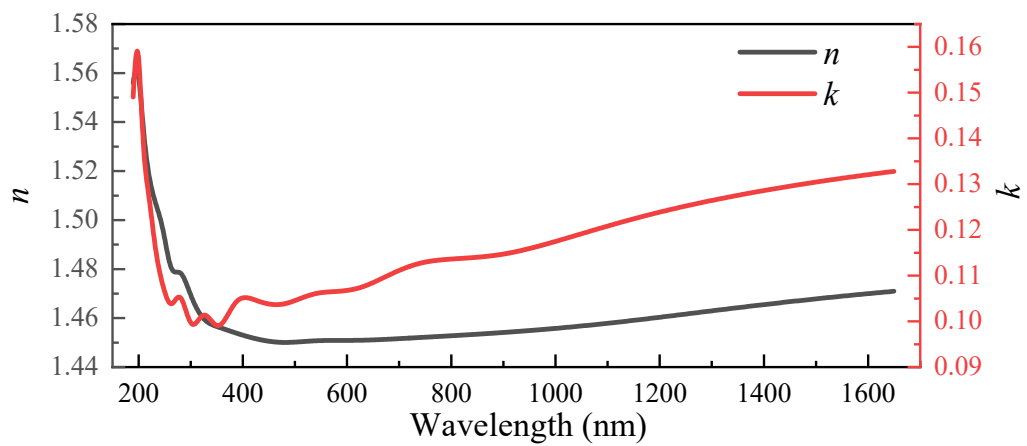


Figure S3: Refractive index n and extinction coefficient k of the inner surface of the shell.

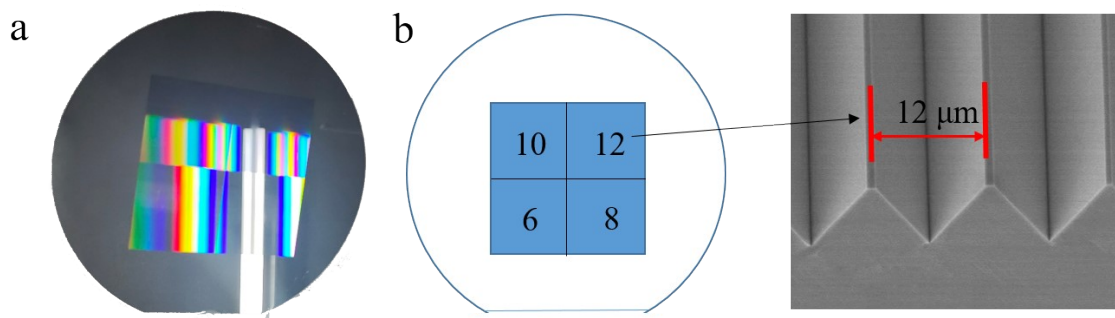


Figure S4: Morphologies of the silicon wafer template. (a) The physical drawing of the silicon wafer template. (b) The schematic diagram of the positions of templates with different structural spaces and the morphology of the silicon wafer template with a space of 12 μm .

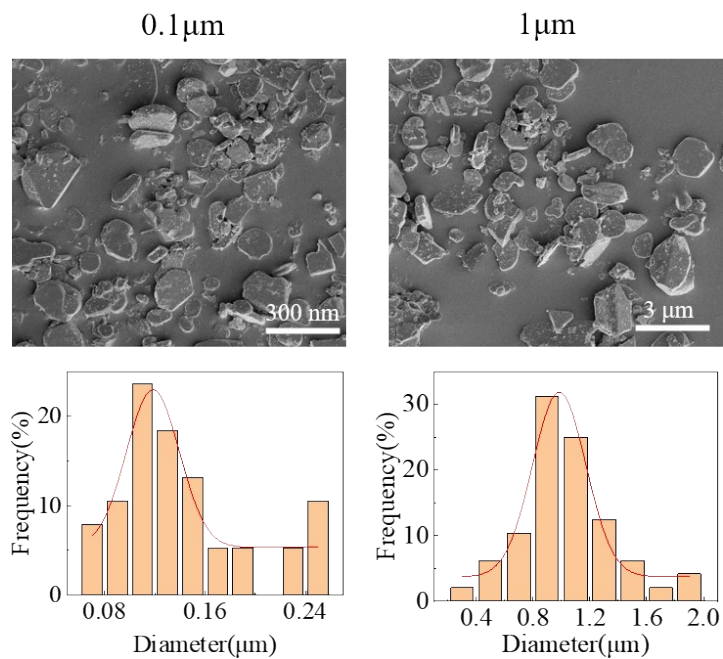


Figure S5: Distribution of Al_2O_3 with different particle sizes.

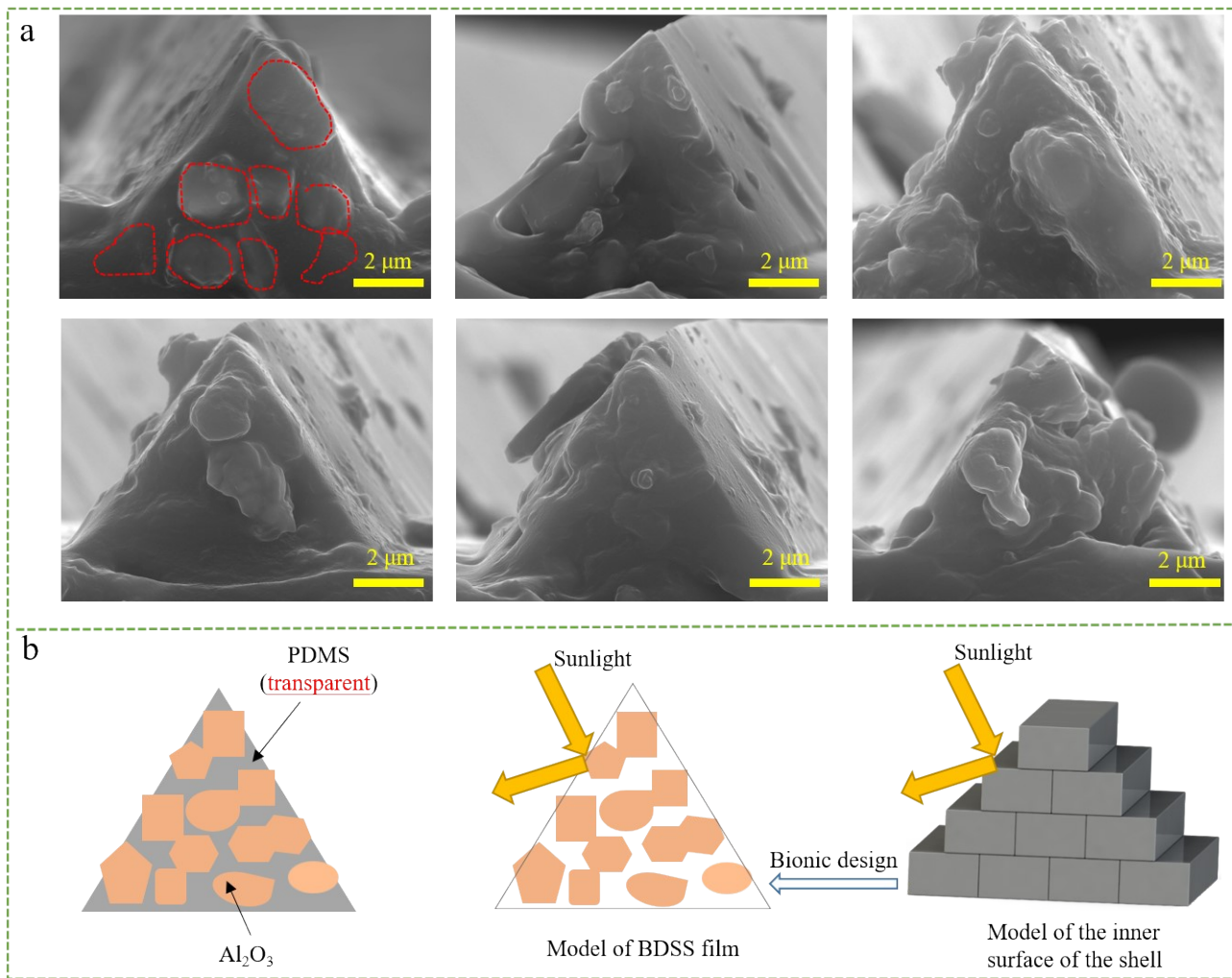


Figure S6: Image characterization and design ideas of BDSS films. (a) SEM images of BDSS films at six different positions. (b) The design concept of BDSS films.

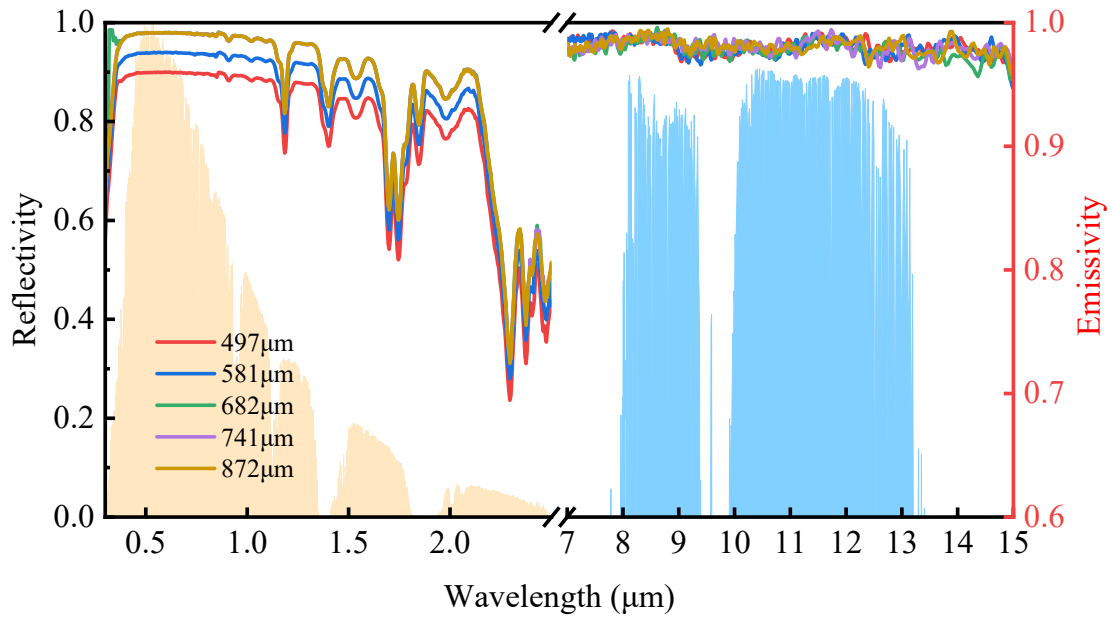


Figure S7: The effect of film thickness on optical properties of the BDSS films.

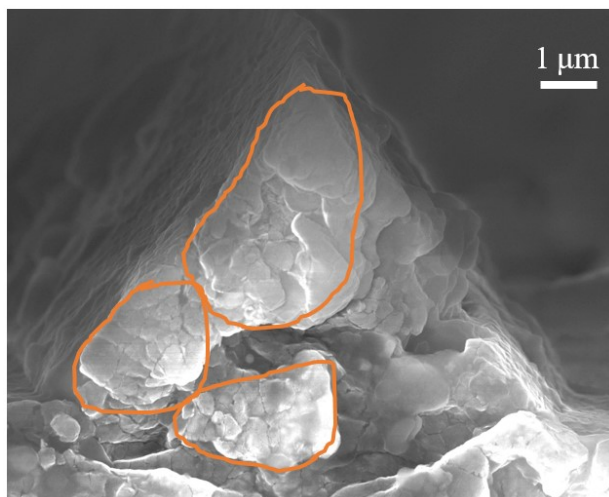


Figure S8: The SEM image of BDSS film with doping particle concentration of 14:10. It can be seen that the particles agglomerate to form large-scale clumps.

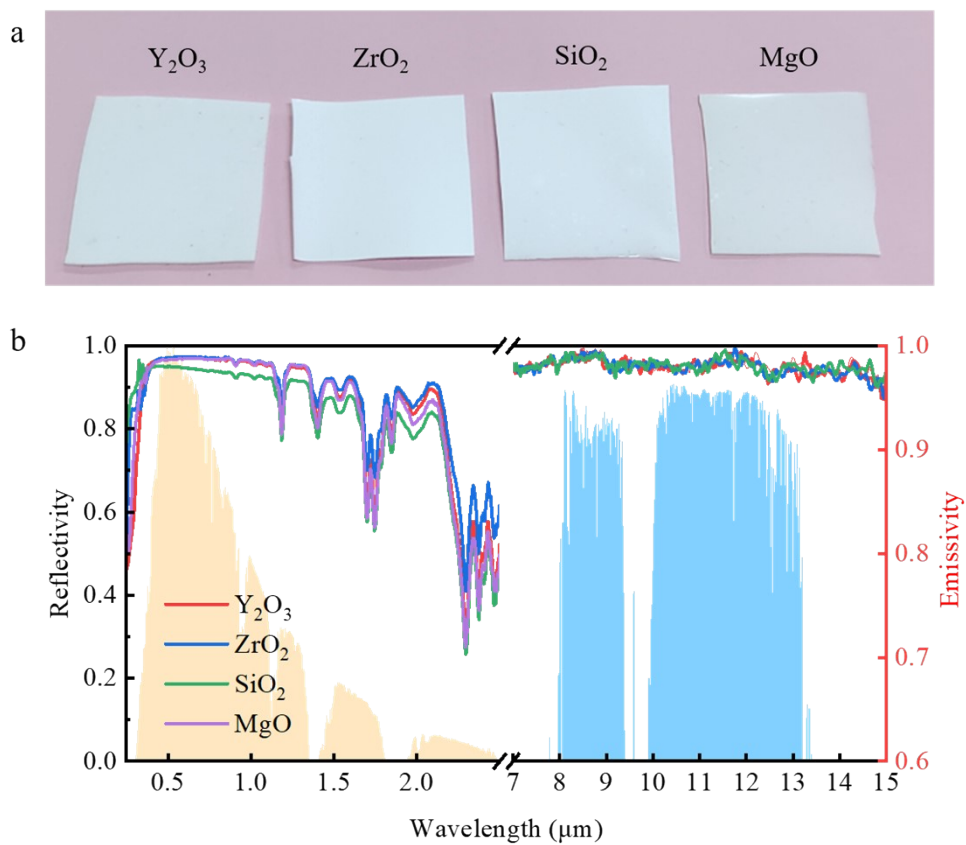


Figure S9: Appearances and reflectance of BDSS films fabricated with different particles. (a) Appearances of BDSS films fabricated with Y_2O_3 , ZrO_2 , SiO_2 , and MgO , respectively. (b) Optical characteristics of BDSS films fabricated with Y_2O_3 , ZrO_2 , SiO_2 , and MgO .

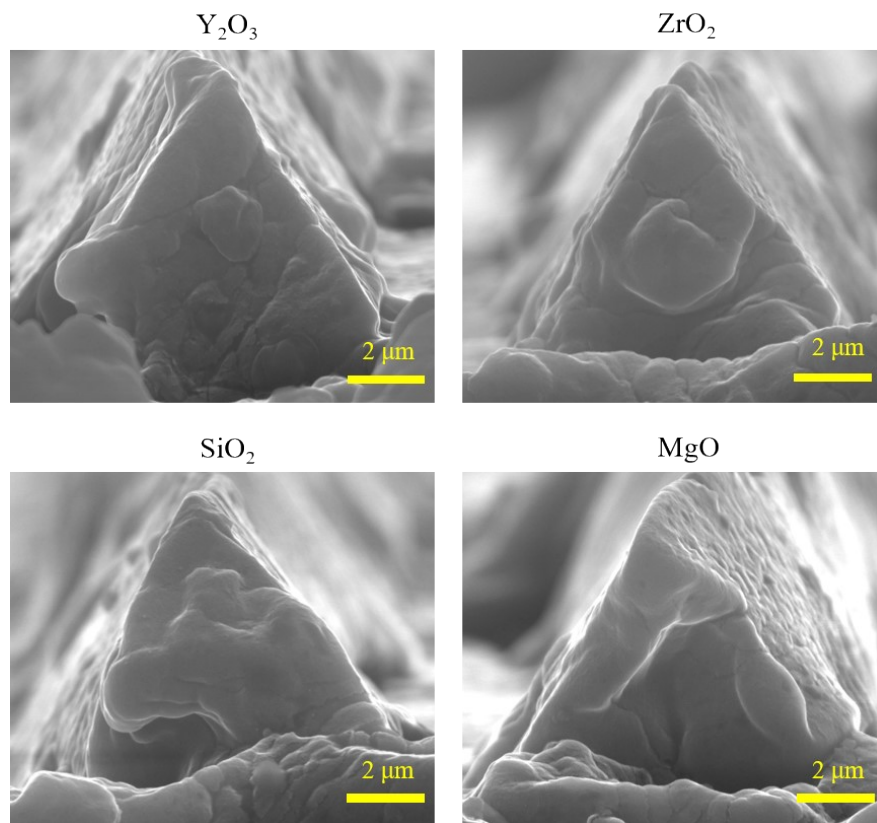


Figure S10: SEM images of BDSS films fabricated with Y_2O_3 , ZrO_2 , SiO_2 , and MgO .



Figure S11: Cooling device physical map. From left to right, there is polystyrene foam supported by stool, multi-channel thermometer, hygrometer, and solar power meter.

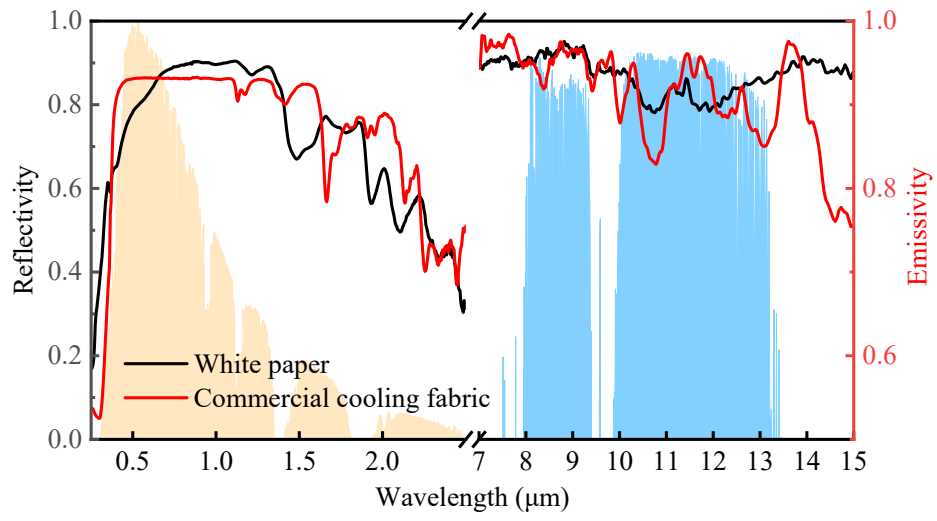


Figure S12: Optical properties of white paper and commercial cooling fabric.

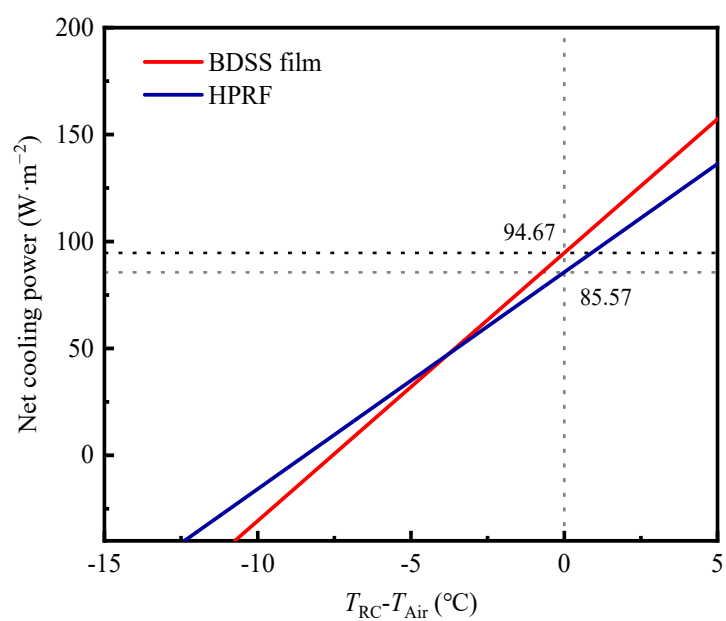


Figure S13: Net cooling power of the BDSS film and HPRF. The results showed that the net cooling power of the BDSS film was 94.67 W/m², while the net cooling power of the HPRF was only 85.57 W/m².

Section 2. Supplementary Video S1

Video S1. Flexibility test of BDSS film.